

Amplitude Factorization in the Electroweak Standard Model

Simon Plätzer

*Institute of Physics, NAWI Graz, University of Graz, Universitätsplatz 5, A-8010 Graz, Austria
Particle Physics, Faculty of Physics, University of Vienna, Boltzmannngasse 5, A-1090 Wien, Austria and
Erwin Schrödinger Institute for Mathematics and Physics, University of Vienna, A-1090 Wien, Austria*

Malin Sjö Dahl

*Department of Physics, Lund University, Box 118, 221 00 Lund, Sweden and
Erwin Schrödinger Institute for Mathematics and Physics, University of Vienna, A-1090 Wien, Austria*

(Dated: July 16, 2024)

We lay out the basis of factorization at the amplitude level for processes involving the entire Standard Model. The factorization appears in a generalized eikonal approximation in which we expand around a quasi-soft limit for massive gauge bosons, fermions, and scalars. We use the chirality-flow formalism to express loop exchanges or emissions as operators on chiral structures. This forms the basis for amplitude evolution with parton exchange and branching in the full Standard Model, including the electroweak sector.

I. INTRODUCTION

The measurements and searches for new physics at current and future colliders operate through observables which resolve widely different energy scales between the hard scattering and the details of the observed final state. Such observables, which we generally refer to as infrared sensitive, are computable in perturbation theory, however, the appearance of large logarithms of the scale ratios and other resolution parameters invalidates the truncation of the perturbative series at any fixed order in the (small) coupling parameter. Instead, resummation — which is unavoidably tied to the description of multiple emissions and properties of large multiplicity final states — is required to capture the physical behavior.

Resummation is only possible if factorization takes place, *i.e.* when we can build up scattering amplitudes with many emissions and exchanges of the interacting particles from repeated simple and universal building blocks. This is well understood in the context of the strong interaction (see *e.g.* [1]), and has paved the way for the description of jets, and ultimately the development of versatile simulations of high energy collisions (see *e.g.* [2]). While the strong interaction, described by Quantum Chromodynamics (QCD), contributes the bulk of the complexity in hadronic final states, at high enough energies there is no kinematic suppression mechanism for electroweak interactions. All Standard Model degrees of freedom need to be taken into account to reliably predict the details of the final states in which we strive to observe deviations from the Standard Model at colliders.

In this paper, we outline a formalism which serves as the basis for generalizing soft gluon evolution [3–10] and amplitude level parton branching [11, 12]. Our formalism also accounts for the exchange and emission of electroweak bosons, along with additional effects from the electroweak interaction of the fermions in the Standard Model. This will allow us to describe observables which are sensitive to changes in the isospin composition of

emitting systems, as well as to account for the chiral nature of the electroweak interactions. Our work will provide the fundamental building blocks to apply and extend amplitude level evolution to the resummation of electroweak effects [13–18]. It will also provide a thorough framework for the construction of parton branching algorithms which coherently treat electroweak and QCD effects on equal footing. Our framework will complement existing approaches of electroweak showers [19–21] which are based on emission amplitudes only [22] and will link to electroweak evolution for strictly high energies in the quasi-collinear limit, *e.g.* [23, 24]. It is also in shape to include the effects of mixing, decays and the projection onto observed states as outlined in [25]. The latter can lead to possible cancellations of logarithmically enhanced contributions [26] or to mechanisms restoring the cancellation [27].

We focus in particular on the underlying kinematic region in which factorization, including different mass shells and possibly recoils, take place, and on the structure of the evolving amplitude as a vector in the space of isospin and chiral structures, similar to how it is typically described as a vector in color space. This will form the basis of an actual implementation of an evolution algorithm within amplitude evolution frameworks such as the `CVolver` [7, 9] library.

We first set the notation in section II. The basis of the factorization of fully massive amplitudes is described in section III, with the kinematics facilitating the factorization detailed in section III A. Self-energy insertions, wave function renormalization and cutting of unresolved lines is discussed in section III C, and in section IV the factorization is complemented with a complete flow picture, entailing chiral and isospin structures. Finally we conclude in section V.

II. NOTATION

Central to our analysis is the formalism of treating amplitudes as abstract vectors in a space of tensor structures of (internal) quantum numbers, *i.e.* color, isospin and spinor indices. In order to set the notation for this we start with a simple example: Consider $q(1)Q(2) \rightarrow q(3)Q(4)$ scattering via a gluon exchange, then the amplitude would be written as

$$\mathcal{M} = G u_{i_1, I_1, \alpha}(p_1) u_{i_2, I_2, \gamma}(p_2) \bar{u}_{\beta}^{i_3, I_3}(p_3) \bar{u}_{\delta}^{i_4, I_4}(p_4) \times (t^a)^{i_1}_{i_3} (t^a)^{i_2}_{i_4} \delta_{I_3}^{I_1} \delta_{I_4}^{I_2} (\overline{P_{c_1}} \gamma^\mu P_{c_3})_{\beta\alpha} (\overline{P_{c_2}} \gamma_\mu P_{c_4})_{\delta\gamma}, \quad (1)$$

where $i_{1..4}$ are the color indices, $I_{1..4}$ are the isospin indices, and $c_{1..4}$ are the chiralities we obtain after applying chiral projectors P_c to the external quark lines, and $\alpha, \beta, \gamma, \delta$ are spinor indices. G collectively denotes all other coupling, symmetry factors and propagator denominators. The external wave functions carry explicit momenta, and will specify explicit quantum numbers like spin to be measured (which we have suppressed for readability). We will write this amplitude as

$$|\mathcal{M}\rangle = G |T\rangle, \quad \mathcal{M} = \langle\psi|\mathcal{M}\rangle \quad (2)$$

such that the tensor structure is contained in $|T\rangle$, and explicit color, isospin and chirality is carried by

$$\langle\psi| = u_{i_1, I_1, \alpha}(p_1) u_{i_2, I_2, \gamma}(p_2) \bar{u}_{\beta}^{i_3, I_3}(p_3) \bar{u}_{\delta}^{i_4, I_4}(p_4) \langle\{i_1, \dots\}, \{I_1, \dots\}, \{\alpha, \dots\}\rangle, \quad (3)$$

which signifies an abstract version of the external wave function. The components of the tensor T in terms of explicit indices are recovered by

$$\langle\{i_1, \dots\}, \{I_1, \dots\}, \{\alpha, \dots\}|T\rangle = (t^a)^{i_1}_{i_3} (t^a)^{i_2}_{i_4} \delta_{I_3}^{I_1} \delta_{I_4}^{I_2} (\overline{P_{c_1}} \gamma^\mu P_{c_3})_{\beta\alpha} (\overline{P_{c_2}} \gamma_\mu P_{c_4})_{\delta\gamma}. \quad (4)$$

III. STRATEGY OF FACTORIZATION

We consider a subset of diagrams (which we label by the symbolic index s) for a certain process in which m lines with unresolved particles of flavors $\{g_i\}_m$ carry ‘soft’ momenta $\{k_i\}_m$, and are emitted from, or exchanged in-between, a subset h_s of the n other external lines of flavors $\{f_i\}_n$, which carry ‘hard’ momenta $\{q_i\}_n$. The sub-diagrams involving the emissions and exchanges will then attach to an amplitude with on- or off-shell lines of flavor $\{f'_i\}_n$, which carry momenta $P_{i,s} = q_i + K_{i,s}$, with $K_{i,s}$ being some linear combination of the emitted and exchanged momenta if $i \in h_s$, and $P_{i,s} = q_i$ if $i \notin h_s$ is an external line not connecting to an unresolved line.

Having singled out a certain subgraph from the amplitude as described above, we can write it as

$$\begin{aligned} & | \mathcal{M}_{\{f_i\}_n, \{g_i\}_m}(\{q_i\}_n; \{k_i\}_m) \\ &= \sum_{\{f'_i\}_n} \sum_s \mathbf{R}_s^{\{f'_i\}_n}(\{q_i\}_n; \{k_i\}_m) \\ & \prod_{i \in h_s} \frac{\mathbf{P}_i(q_i + K_{i,s}, M_i)}{(q_i + K_{i,s})^2 - M_i^2} |\mathcal{M}_{\{f'_i\}_n}(\{P_i\}_n)\rangle + \dots \end{aligned} \quad (5)$$

in which \mathbf{P}_i represents the propagator numerator of the hard, off-shell line i as an operator in the space of the involved quantum numbers, and \mathbf{R}_s encodes the remaining structure we intend to factor from the hard process amplitude, *i.e.* \mathbf{R}_s contains all couplings, numerator structures and gauge structures, except the numerators of the hard propagators \mathbf{P}_i attaching to it. This factorization (in eq. (5)) — which has not yet used any approximation — can be diagrammatically represented as

$$|\mathcal{M}_{n+m}\rangle = \sum_s |\mathcal{M}_n\rangle \mathbf{R}_s + \dots \quad (6)$$

where wavy lines denote unresolved particles, $P_{i,s} = q_i + K_{i,s}$ and the ellipse with \mathbf{R}_s refers to topologies which do not factor separately onto the n -parton amplitude.

Our aim is to identify when — in a very general setting — this amplitude factors in a systematically expandable way onto an *on-shell* hard amplitude after isolating external sub-diagrams as above.

We also discuss how we can construct bases for the space of chiral structures such that we can express the abstract operators in a concrete fashion and iterate virtual exchanges and emissions in the solution to an evolution equation of the amplitude.

A. Kinematics

Before we address the more complicated electroweak case, let us recall how soft factorization in QCD works. In this case we would consider emissions and exchanges which contribute a total momentum $K_{i,s}$ to an off-shell line i , carrying a total momentum $P_{i,s} = q_i + K_{i,s}$, where q_i is the on-shell external momentum. Thus

$$\frac{\mathcal{M}(P_{i,s})}{P_{i,s}^2 - M_i^2} = \frac{\mathcal{M}(q_i + K_{i,s})}{2q_i \cdot K_{i,s} + K_{i,s}^2}, \quad (7)$$

which follows from $q_i^2 = M_i^2$. In the uniform soft limit, $K_{i,s} \rightarrow \lambda K_{i,s}$, we differentiate w.r.t. λ to get the power

expansion in λ

$$\frac{\mathcal{M}(P_{i,s})}{P_{i,s}^2 - M_i^2} \rightarrow \frac{1}{\lambda} \frac{\mathcal{M}(q_i)}{2q_i \cdot K_{i,s}} + \frac{2q_i \cdot K_{i,s} (K_{i,s}^\mu \partial_\mu \mathcal{M}(q_i)) - K_{i,s}^2 \mathcal{M}(q_i)}{4(q_i \cdot K_{i,s})^2} + \mathcal{O}(\lambda) . \quad (8)$$

Going back to eq. (7), we note that we can alternatively parametrize the hard momentum q_i by a different hard direction p_i on the same mass-shell,

$$q_i^\mu = p_i^\mu - K_{i,s}^\mu + \frac{K_{i,s} \cdot (K_{i,s} - 2p_i)}{2n \cdot (K_{i,s} - p_i)} n^\mu \quad (9)$$

with a light-like reference vector n , constrained only by $n \cdot (K_{i,s} - p_i) \neq 0$. The above expression essentially serves to obtain $q_i^2 = p_i^2 = M_i^2$ while

$$q_i + K_{i,s} = p_i + (\text{recoil paramter})n , \quad (10)$$

allowing us to expand around a new, on-mass-shell, hard direction p_i , irrespective of the mass-shell condition on $K_{i,s}$ or precisely the way we define a 'soft' $K_{i,s}$. All that matters is that the recoil parameter is small,

$$|2p_i \cdot K_{i,s} - K_{i,s}^2| \ll |n \cdot (p_i - K_{i,s})| \quad (11)$$

such as to obtain an on-shell amplitude from expanding

$$\frac{\mathcal{M}(P_{i,s})}{P_{i,s}^2 - M_i^2} = \frac{n \cdot (p_i - K_{i,s})}{n \cdot p_i} \frac{\mathcal{M}(p_i + (\dots)n)}{2p_i \cdot K_{i,s} - K_{i,s}^2} . \quad (12)$$

In fact, for the soft gluon case above the new parametrization will lead to a similar leading-power expansion as $K_{i,s} \rightarrow \lambda K_{i,s}$, $\lambda \rightarrow 0$,

$$\frac{\mathcal{M}(P_{i,s})}{P_{i,s}^2 - M_i^2} \rightarrow \frac{1}{\lambda} \frac{\mathcal{M}(p_i)}{2p_i \cdot K_{i,s}} + \mathcal{O}(\lambda^0) , \quad (13)$$

with $q_i = p_i + \mathcal{O}(\lambda)$, however it will differ at subleading power.

The aim of our work is thus to make the above procedure an exact parametrization which we can use for a leading power expansion, subject to an explicit Eikonal propagator, including a possible change of mass shell between the emitter momentum before and after the emission, $p_i^2 \neq q_i^2$, and subject only to maintaining momentum conservation of all momenta attached to the amplitude.

As seen, in general the parametrization of the kinematics is complicated by the mass-shell conditions. We consider $q_i^2 = m_i^2$ for the external particles, while the particles propagating along the off-shell lines have masses M_i (as they may well have other flavors). We note that these masses refer to *physical, on-shell masses*, a choice which will provide us with a factorization of physical, renormalized S-matrix elements [28].

On top of this, we need to allow for the possibility to implement recoil to respect overall energy-momentum conservation.

To understand the kinematic regions where the factorization is applicable, we consider a frame where the off-shell momentum, directly to the right of the big gray blob on the the right-hand side in eq. (6), is approximated by

$$p_i = \left(\sqrt{E_i^2 + M_i^2}, \vec{0}_\perp, E_i \right) \quad (14)$$

with $p_i^2 = M_i^2$, while $P_{i,s}^2 \neq M_i^2$.

We then introduce a light-like momentum $n_{i,s}$ with a direction which maximizes $p_i \cdot n_{i,s}$,

$$n_{i,s} = \frac{n_{i,s} \cdot p_i}{E_i + \sqrt{E_i^2 + M_i^2}} \left(1, \vec{0}_\perp, -1 \right) . \quad (15)$$

Any additional deviation from the four-momentum p_i we write in terms of

$$Q_{i,s} = \left(Q_{i,s}^{(+)} + Q_{i,s}^{(-)}, \vec{Q}_{i,s}^{(\perp)}, Q_{i,s}^{(+)} - Q_{i,s}^{(-)} \right) . \quad (16)$$

With this in mind, we express the external momenta q_i and the $K_{i,s}$ in a covariant way as

$$K_{i,s}^\mu = \Lambda^\mu{}_\nu \left(Q_{i,s}^\nu + \delta_{i,s} n_{i,s}^\nu \right) \quad (17)$$

$$q_i^\mu = \Lambda^\mu{}_\nu \left(\alpha p_i^\nu + \frac{(1 - \alpha^2) M_i^2 + p_i \cdot Q_{i,s}}{2\alpha n_{i,s} \cdot p_i} n_{i,s}^\nu \right) - K_{i,s}^\mu ,$$

where the parameter $\delta_{i,s}$ is determined such that $q_i^2 = m_i^2$, giving

$$\delta_{i,s} = \frac{(M_i^2 \alpha^2 - m_i^2 + (1 - 2\alpha) p_i \cdot Q_{i,s} + Q_{i,s}^2)}{2n_{i,s} \cdot (\alpha p_i - Q_i)} - \frac{n_{i,s} \cdot Q_{i,s} (M_i^2 (1 - \alpha^2) + p_i \cdot Q_{i,s})}{2\alpha n_{i,s} \cdot p_i n_{i,s} \cdot (\alpha p_i - Q_i)} , \quad (18)$$

whereas the parameter α , as well as the boost itself, relates to maintaining energy and momentum conservation, as discussed below.

For the momenta not involved in the exchange or emission (i.e., legs not in h_s), setting $Q_{i,s} = 0$ and $M_i^2 = m_i^2$ in eq. (17) gives

$$q_i^\mu = \Lambda^\mu{}_\nu \left(\alpha p_i^\nu + \frac{(1 - \alpha^2) m_i^2}{2\alpha n_{i,s} \cdot p_i} n_{i,s}^\nu \right) . \quad (19)$$

Note that, if emissions are involved, the $K_{i,s}$ are some combination of emission and exchange momenta, which satisfy $\sum_{i \in h_s} K_{i,s} = \sum_I k_i$ where the right hand sum is over all emissions. Thus the total outgoing momentum of our process, Q , is

$$Q^\mu = \sum_i k_i^\mu + \sum_i q_i^\mu = \alpha \Lambda^\mu{}_\nu \left(\sum_i p_i^\nu + \frac{1 - \alpha^2}{\alpha^2} \underbrace{\sum_i \frac{M_i^2}{2n_{i,s} \cdot p_i} n_{i,s}^\nu}_{\equiv N_1^\nu} + \frac{1}{\alpha^2} \underbrace{\sum_{i \in h_s} \frac{p_i \cdot Q_{i,s}}{2n_{i,s} \cdot p_i} n_{i,s}^\nu}_{\equiv N_2^\nu} \right) . \quad (20)$$

In order to implement four-momentum conservation the Lorentz transformation and scaling parameter α need to obey

$$(\Lambda^{-1})^\nu{}_\mu Q^\mu = \alpha Q^\nu + \frac{1 - \alpha^2}{\alpha} N_1^\nu + \frac{1}{\alpha} N_2^\nu \quad (21)$$

which fixes α by requiring the same invariant mass before and after the Lorentz transformation.

Demanding that $\alpha > 0$, and $\alpha \rightarrow 1$ if all masses M_i , and the momenta $Q_{i,s}$ vanish, we find (cf. eq. (17)) a solution which in general admits $\alpha = 1 + \mathcal{O}(\lambda)$ as $p_{i,s} \cdot Q_{i,s} \rightarrow \lambda p_{i,s} \cdot Q_{i,s}$, $\lambda \rightarrow 0$, irrespective of the kinematic limit covered by this scaling. Note, however, that we have not constrained the form of the Lorentz transformation (in particular it need not be small), and in general only use

$$\begin{aligned} q_i^\mu &= \Lambda^\mu{}_\nu \left(p_i^\nu - \tilde{K}_{i,s}^\nu + \mathcal{O}(\lambda) \right) \\ K_{i,s}^\mu &= \Lambda^\mu{}_\nu \left(\tilde{K}_{i,s}^\nu + \mathcal{O}(\lambda) \right) \\ \tilde{K}_{i,s}^\nu &= \frac{M_i^2 - m_i^2 + Q_{i,s}^2}{2(p_i \cdot n_{i,s} - n_{i,s} \cdot Q_{i,s})} n_{i,s}^\nu + Q_{i,s}^\nu. \end{aligned} \quad (22)$$

Phase space factorization can be obtained systematically at leading power in λ for such kinematic mappings as shown in [12]. We note that we can uniquely invert the mapping and obtain an expression of $Q_{i,s}$ if we have fixed p_i and $n_{i,s}$. This also means that we can use this definition also when $K_{i,s}$ and $K_{j,s}$ are not independent, *e.g.* for a one-loop exchange in between two legs i and j we have $K_{i,s} = -K_{j,s} = k$. Notice that we have chosen a

backward direction $n_{i,s}$ differently per hard momentum p_i .

The mapping in eq. (17) is designed, such that the denominator of the off-shell propagators are directly given in terms of

$$(q_i + K_{i,s})^2 - M_i^2 = 2p_i \cdot Q_{i,s}, \quad (23)$$

in analogy with eq. (8). Our expansion is thus in

$$p_i \cdot Q_{i,s} \ll p_i \cdot n_{i,s} \equiv S_{i,s} \quad (24)$$

and $\lambda \sim p_i \cdot Q_{i,s}/S_{i,s}$ is our counting parameter which simultaneously enforces the above hierarchy for all hard lines i . It is important to stress that we do not consider different p_i for different classes of diagrams s , while we may want to exploit different parametrizations of unresolved momenta if needed.

B. Factorization

In order to encode the quantum numbers s of external particles (spin, color, isospin, etc.) we introduce an operator corresponding to the on-shell wave functions of the particles we consider,

$$\langle s | \bar{\Psi}(q, m) | s' \rangle = \bar{\psi}_s(q, m) \delta_{ss'}, \quad (25)$$

$$i\Psi(q, m)\bar{\Psi}(q, m) = \mathbf{P}(q, m)|_{q^2=m^2}. \quad (26)$$

In total, this allows us to write, at leading power,

$$\begin{aligned} \left(\prod_{i \notin h_s} \bar{\Psi}_{f_i}(q_i, m_i) \right) \left(\prod_{i \in h_s} \frac{\mathbf{P}_{f'_i}(q_i + K_{i,s}, M_i)}{(q_i + K_{i,s})^2 - M_i^2} \right) | \mathcal{M}_{\{f'_i\}_n}(\{P_i\}_n) \rangle = \\ \left(\prod_{i \in h_s} \frac{\Psi_{f'_i}(\Lambda p_i, M_i)}{2p_i \cdot Q_{i,s}} \right) \times \left(\prod_i \bar{\Psi}_{f'_i}(p_i, M_i) | \mathcal{M}_{\{f'_i\}_n}(\{p_i\}_n) \rangle \right) + \mathcal{O}(\lambda^{-\#h_s+1}), \end{aligned} \quad (27)$$

where $\#h_s$ is the number of hard off-shell legs interacting with unresolved partons. Here we have used that the amplitude contracted with external wave functions is a Lorent invariant. In the light of the kinematics discussion above, we then find that we can factor the amplitude at leading power in λ as

$$|\tilde{\mathcal{M}}(\{q_i\}_n; \{k_i\}_m)\rangle \simeq \sum_s \mathbf{S}_s(\{q\}_{i \in h_s}, \{k_i\}_m) |\tilde{\mathcal{M}}(\{p_i\}_n)\rangle, \quad (28)$$

in terms of the on-shell amplitude with n external hard lines, $|\tilde{\mathcal{M}}\rangle = \prod_i \bar{\Psi}_i |\mathcal{M}\rangle$, carrying momenta $\{p_i\}_n$ (we

have suppressed the flavor labels for the sake of readability). The factored contribution is given by the operator

$$\begin{aligned} \mathbf{S}_{s; \{f_i\}_n, \{g_i\}_m}^{\{f'_i\}_n}(\{q\}_{i \in h_s}, \{k_i\}_m) = i \left(\prod_{j \in h_s} \bar{\Psi}_{f'_j}(q_j, m_j) \right) \\ \times \mathbf{R}_{s; \{f_i\}_n, \{g_i\}_m}^{\{f'_i\}_n}(\{q\}_{i \in h_s}, \{k_i\}_m) \left(\prod_{j \in h_s} \frac{\Psi_{f'_j}(\Lambda p_j, M_j)}{2p_j \cdot Q_{j,s}} \right), \end{aligned} \quad (29)$$

which is to be understood by expressing either q_i or p_i as a function of $Q_{i,s}$, $n_{i,s}$ and p_i or q_i respectively. This is

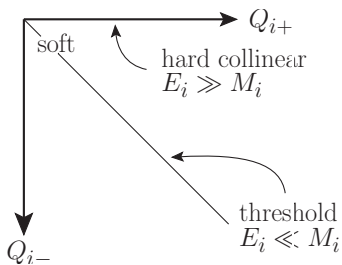


FIG. 1. Illustration of the various regions of validity of our parametrization. As seen from, eq. (30) the condition $p_i \cdot Q_{i,s} \ll p_i \cdot n_{i,s}$ is fulfilled if either both Q_{i+} and Q_{i-} are small (the genuinely soft region) or if $E_i \gg M_i$ and $Q_{i-} \rightarrow 0$ (the hard collinear region) or if $E_i \ll M_i$ and $Q_{i-} \rightarrow -Q_{i+}$ (the threshold region).

possible because the amplitude contracted with external wave functions, $|\tilde{\mathcal{M}}\rangle$, is Lorentz invariant, hence a function of momentum invariants, and can thus be Taylor-expanded around $p_i \cdot Q_{i,s} \rightarrow \lambda p_i \cdot Q_{i,s}$ in the limit $\lambda \rightarrow 0$. Notice that also q_i and the mapped momentum of the exchanges and emissions are proportional to the Lorentz transform which will therefore drop out of the final expression of our effective matrix elements. In essence we achieve factorization by evaluating different parts of the amplitude in different frames. Furthermore, the evaluation of the amplitude may be performed in different frames for different sets s , and the phase space integration may be performed in a third, as long as this difference is not contributing at leading power.

Further simplifications can only occur if we consider stronger constraints on the kinematic limits, though our factorization in this general case serves as a starting point for a formula which interpolates in-between different limits. In terms of our scaled momentum $Q_{i,s}$, the requirement of eq. (24) encompasses kinematic configurations, which are essentially limited by several different regions. They become apparent when one considers, in a specific frame for p_i and $n_{i,s}$, the forward (along p_i) and backward (along $n_{i,s}$) components $Q_{i,s}^{(\pm)}$ and the hard leg's kinetic energy E_i and mass M_i , such that $E_i^2 + M_i^2 \sim S_{i,s}$.

Our expansion is valid if

$$p_i \cdot Q_{i,s} = \sqrt{E_i^2 + M_i^2} (Q_{i,s}^{(+)} + Q_{i,s}^{(-)}) + E_i (Q_{i,s}^{(-)} - Q_{i,s}^{(+)}) \ll p_{i,s} \cdot n_{i,s} = S_{i,s}. \quad (30)$$

The regions of validity contain a Glauber-type region in which $Q_{i,s}$ becomes purely transverse, along with a soft, a hard-collinear, and a threshold region, as depicted in figure 1.

One boundary of the available phase space is the hard (quasi-)collinear region in which $Q_{i,s}^{(-)} \ll S_{i,s}$ but $Q_{i,s}^{(+)}$ is unconstrained and the hard leg is highly energetic, $E_i \gg M_i$. Another limiting region is the threshold region with $E_i \ll M_i$. The regions intersect in the genuine 'soft' region where $Q_{i,s}^{(+)} \sim Q_{i,s}^{(-)} \ll S_{i,s} / \sqrt{E_i^2 + M_i^2}$ i.e., $Q_{i,s}^\mu$

is small compared to the hard scales in all of its components. The 'soft' region also contains a Glauber-type region in which $Q_{i,s}$ becomes purely transverse. In both cases, the exchange or emission momentum $K_{i,s}$ is then accounting for the change in mass-shell between M_i and m_i in its respective forward and backward components. Note that $K_{i,s}$ will in general not be soft in the usual sense, neither in its three-momentum, nor in all of its components. In the quasi-soft limit we will find a generalized Eikonal approximation in which $Q_{i,s}$ is small in all of its components. In this case we can write

$$q_i^\mu = \Lambda^\mu{}_\nu \left(p_i^\nu + \frac{m_i^2 - M_i^2}{2p_i \cdot n_{i,s}} n_{i,s}^\nu + \mathcal{O}(\lambda) \right). \quad (31)$$

Also note that we do not rely on the hard line being highly energetic or close to threshold.

C. Self energy insertions, wave function renormalization, and cutting of unresolved lines

Within our factorization, one would also be tempted to consider the factorization of self-energy insertions which appear as iterations of

$$\frac{\mathbf{P}_{f'_i}(q_i + K_{i,s}, M'_i)}{(q_i + K_{i,s})^2 - M_i'^2} \Sigma_{f'_i f_i}(q_i + K_{i,s})$$

on the leg with momentum $q_{i,s} + K_{i,s}$ in the figure in eq. (6), or on a corresponding emission process. Note that the self energy $\Sigma_{f'_i f_i}$ is an operator in the space of quantum numbers, as well. Multiple insertions, however, are not separated in scale, but contribute equally at leading power with the same propagator attached and therefore show no hierarchy. Contributing propagators from different intermediate particles would appear to be suppressed if the masses of the mixing particles are different, $(q_i + K_{i,s})^2 - M_i'^2 = 2p_i \cdot Q_{i,s} + M_i^2 - M_i'^2$, however propagators which resum these effects develop poles at the mass shells of all particles involved in the mixing. This necessarily leads us to consider resummed propagators and a proper relation to physical masses. In fact, as highlighted above, we parametrize the kinematics in terms of the physical masses m_i and M_i . In this case, the propagator denominators, for a complex mass scheme [29, 30], are expressed in terms of the renormalized (complex) mass parameters $M_{i,R}^2$ and renormalized self energy contributions $\Sigma_{i,R}$, where the physical mass is a solution to $M_i^2 = M_{i,R}^2 + \Sigma_{i,R}(M_i^2)$. Our mapping has the virtue that

$$\frac{1}{(q_i + K_{i,s})^2 - M_{i,R}^2 - \Sigma_{i,R}((q_i + K_{i,s})^2)} = \frac{1}{\lambda} \frac{1}{2p_i \cdot Q_{i,s}} \frac{1}{1 - \Sigma'_{i,R}(M_i^2)} + \mathcal{O}(1) \quad (32)$$

as $p_i \cdot Q_{i,s} \rightarrow \lambda p_i \cdot Q_{i,s}$, $\lambda \rightarrow 0$, thus providing the proper wave function renormalization to the hard amplitude we

factor to, and the legs involved in the contributions we do intend to factor from the amplitude. Residues of mixing propagators can then be accounted for in the exchange or emission kernels together with the elementary vertex. Beyond the leading order, the \mathbf{S} operator will thus be provided with the relevant wave function renormalization constants and as such is defined beyond the lowest order. This holds for all internal lines we consider here (scalar, fermion, vector), as well as for unstable particles when using a complex mass scheme.

Another consequence is that the program of casting virtual corrections into phase space type integrals to locally cancel infrared enhancements from the real emission (as *e.g.* systematized in [10]) thus faces an important modification: Instead of an on-shell cut through the unresolved, ‘soft’, exchanges we will need to use a cutting rule

$$\frac{1}{k^2 - m^2 - im\Gamma \operatorname{sign}(T \cdot k)} = \frac{1}{k^2 - m^2 + im\Gamma} + 2i \frac{m\Gamma}{(k^2 - m^2)^2 + m^2\Gamma^2} \theta(T \cdot k). \quad (33)$$

This identity has a straightforward physical interpretation: while it clearly yields the standard cut result for $\Gamma \ll m$, it instructs us for the finite-width case to replace the cut with a Breit-Wigner factor, and cuts through the decay products of the exchanged unstable particle, noting that $2m\Gamma$ is the exchanged particle’s decay matrix element integrated over phase space. Unitarity as a building block of parton branching and resummation algorithms thus appears in a different form, though this poses no conceptual problem if one treats subtraction terms for real and virtual corrections separately, and performs a careful analysis of measurements [25]. The latter also will project onto decays of the unstable physical bosons after their high energy evolution.

IV. A COMPLETE FLOW PICTURE

In this section, we discuss (flow) versions of the bases for color, chirality and isospin, to be used in eq. (1).

For the color structure, it is well known how to employ the Fierz identity to decompose all color structure into flows, see for example [7, 9, 10, 31, 32]. We remark, that while this paper focuses on flow representations, one can of course also use other decompositions. In particular for color structure, orthogonal bases can be used [33–35], a context in which there has recently been significant development [36, 37].

For isospin, we note that the chiral states allow us to work directly with eigenstates of the isospin operator. At high energies, in the unbroken phase, one could treat $SU(2)_L$ in terms of flows, as for any $SU(N)$. However, as we want to treat the weak bosons as mass eigenstates, we instead propose to simply work with explicit weak isospin eigenstates. Hypercharge comes from an abelian $U(1)$ and therefore does not come with any flow representation.

Also the chiral structures from spin and momenta can be decomposed into flows by employing the Fierz identity on the spinors, a simplification which is built into the Feynman rules of chirality flow. We note however, that for a complete reduction in terms of *tensor structures* we need more flows than just the direct contraction between external spinors. As we will see, this means that the tensor flow basis for chiral structures comes with more terms than the flow basis for color.

Overall, Fierz rearrangements will thus allow us to obtain a basis of (tensor) structures for quantities like $(t^a)^{i_1}_{i_3} (t^a)^{i_2}_{i_4} \delta_{I_3}^{I_1} \delta_{I_4}^{I_2} (\overline{P_{c_1}} \gamma^\mu P_{c_3})_{\beta\alpha} (\overline{P_{c_2}} \gamma_\mu P_{c_4})_{\delta\gamma}$ such that we can express the amplitude in a basis of flows, $|\sigma\rangle$,

$$|T\rangle = \sum_{\sigma} c_{\sigma} |\sigma\rangle, \quad (34)$$

$$|\mathcal{M}\rangle = \sum_{\sigma} \mathcal{M}_{\sigma} |\sigma\rangle, \quad (35)$$

with $\mathcal{M}_{\sigma} = G c_{\sigma}$ in our simple example from the introduction, Sec. II, though more general and non-trivial mixtures of kinematic dependence will multiply each flow vector in the case of general amplitudes.

A. A flow basis for chiral structures

The chiral nature of the electroweak interaction, and the relevance of spin correlations, call for a flow concept which we will introduce now: In analogy with performing resummation in color space using a spanning set of color flows, we will prove that the resummation evolution in Lorentz space can be described using ‘chirality flows’. We thus build on the chirality-flow formalism [38–42], which allows the immediate translation of Feynman diagrams to spinor inner products.

We therefore describe particles in terms of their chirality, and expect a decomposition of the full amplitude (with both left- and right helicity) to chirality to have been performed before the start of the evolution. To be precise we want to choose a basis for the amplitude vector written as a vector in our abstract formalism above, $\langle\langle \{i_1, \dots\}, \{I_1, \dots\}, \{\alpha, \dots\} | \mathcal{M} \rangle\rangle$, where $|\mathcal{M}\rangle$ is the amplitude without the external wave functions (*cf.* a color flow without assigned external colors) and we will work out the action of the factored diagrams using eq. (26). In this way, we will gain full analytic control of the Lorentz structure.

Denoting a left-chiral fermion with momentum p_i with $|i\rangle = \textcircled{\leftarrow} \text{---} i$ (or $[i] = \textcircled{\leftarrow} \text{---} i$) and a right-chiral fermion with $|j\rangle = \textcircled{\rightarrow} \text{---} j$ (or $\langle j| = \textcircled{\rightarrow} \text{---} j$) we want to consider the effect of (say) a photon exchange between two — for now massless — fermions. The effect of mass will be considered below.

Representing the Lorentz structure $p_\mu \sigma^\mu$ with a ‘‘momentum dot’’ $p_\mu \sigma^\mu = \begin{array}{c} p \\ \dashrightarrow \bullet \dashrightarrow \end{array}$, and similarly $p_\mu \bar{\sigma}^\mu = \begin{array}{c} p \\ \dashrightarrow \bullet \dashleftarrow \end{array}$, we have, for an exchange between two legs, the chiral structure (drawn in black on top of a gray Feynman diagram) to the left below for two left-chiral fermions and the structure to the right if i is left-chiral, and j is right-chiral

$$\cdot \quad (36)$$

Here, to the left, the dashed line connecting the outgoing particles i and j is the graphical representation of the spinor inner product $[j i]$. After the exchange, the particles i and j are thus connected by a ‘‘chirality flow’’. The momentum dots connect somewhere within the blob and (naively) complicates the chirality structure of the rest of the diagram. However, as we will show below, a complete set of chirality-flow structures connecting the external spinors can be given by considering the contractions

$$(37)$$

for some four-vector p contracted with $\sigma/\bar{\sigma}$, and some antisymmetric rank two tensor $A_{\mu\nu}$ contracted with $\frac{1}{2}(\sigma^\mu \bar{\sigma}^\nu - \sigma^\nu \bar{\sigma}^\mu)$, and for connections between all pairs of external particles. Before the exchange, the particles i and j to the left in eq. (36) were thus contracted to some (other) external particles via these structures.

After the exchange, the chirality flows (of the type in eq. (37)) to which i and j were contracted, will be connected to each other via the double momentum-dot structure in the left diagram. This gives rise to structures with up to 2+2+2 Lorentz index contractions (in case i and j connected to two different chirality-flow structures of type $\dashrightarrow \bullet \dashrightarrow$).

In case the external particles have opposite chirality, we will have a chirality flow of the type to the right in eq. (36), giving rise to two momentum dot structures of up to 2+1 Lorentz indices (if i and j were originally chirality-flow connected to say i' and j' respectively via $i' \dashrightarrow \blacksquare \dashleftarrow i$, $j \dashrightarrow \blacksquare \dashleftarrow j'$, or connected to each other via $j \dashrightarrow \bullet \dashleftarrow i$).

We will now argue that in both cases, the structures can be simplified back to the cases in eq. (37). We also schematically derive the decomposition of structures with up to six momentum dots which can appear in intermediate steps.

First, we note that the usage of $\langle i j \rangle$, $[i j]$; $p_\mu [i |\sigma^\mu |j]$, $p_\mu \langle i |\bar{\sigma}^\mu |j \rangle$ and $A_{\mu\nu} \langle i |\bar{\sigma}^{\mu\nu} |j \rangle$, $A_{\mu\nu} \langle i |\sigma^{\mu\nu} |j \rangle$ for some antisymmetric tensor $A^{\mu\nu}$, is equivalent to the decomposition of products of

γ -matrices into 1 and γ^5 (via the decomposition into left and right chiral states); γ^μ , $\gamma^5 \gamma^\mu$ and $[\gamma^\mu, \gamma^\nu]$ respectively.

In principle this is in itself a proof that these are the structures to anticipate. Nevertheless we will explicitly prove that the action of gauge boson exchange, starting from any of these structures, will result in linear combinations of the same spanning structures. That this holds for exchange of fermions and scalars then follows trivially. We start with considering the simplest case when two momentum dots, for example coming from the fermion propagators (slashed momenta) arising by photon exchange, are attached to the same chirality-flow line. Using the chirality-flow Feynman rules from [38], we obtain

$$(38)$$

i.e. the partners i' and j' (originally connected to i and j respectively) become chirality-flow connected, whereas i and j instead becomes connected to each other. To decompose the two momentum dots into our basis, we use the identity

$$\sigma^\mu \bar{\sigma}^\nu = g^{\mu\nu} + \frac{1}{2}(\sigma^\mu \bar{\sigma}^\nu - \sigma^\nu \bar{\sigma}^\mu). \quad (39)$$

Contracting with external momenta p_1 and p_2 , and sandwiching between external spinors this gives

$$\begin{aligned} \underbrace{[i | p_{1\mu} p_{2\nu} \sigma^\mu \bar{\sigma}^\nu | j]}_{\equiv i \dashrightarrow \bullet \dashrightarrow j} &= p_1 \cdot p_2 \underbrace{[i j]}_{\equiv i \dashrightarrow \bullet \dashrightarrow j} \\ &+ \underbrace{[i | p_{1\mu} p_{2\nu} \frac{1}{2}(\sigma^\mu \bar{\sigma}^\nu - \sigma^\nu \bar{\sigma}^\mu) | j]}_{\equiv i \dashrightarrow \blacksquare \dashrightarrow j} \end{aligned} \quad (40)$$

(applied to i' and j'). We remark that it is the antisymmetric part of $p_{1\mu} p_{2\nu}$, $\frac{1}{2}(p_{1\mu} p_{2\nu} - p_{1\nu} p_{2\mu})$, that survives the contraction in the second term; more generally, we find an antisymmetric rank-2 tensor contracted with $\frac{1}{2}(\sigma^\mu \bar{\sigma}^\nu - \sigma^\nu \bar{\sigma}^\mu)$.

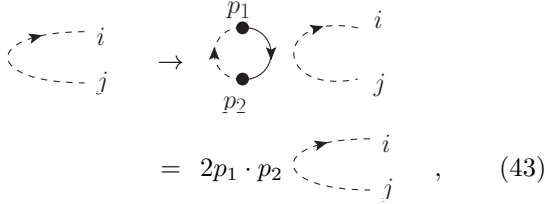
Exploring the effect on the basis vector we obtain

$$(41)$$

with

$$(A_{12})_{\mu\nu} = \frac{1}{2}(p_{1\mu}p_{2\nu} - p_{1\nu}p_{2\mu}), \quad (42)$$

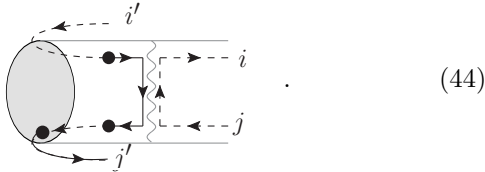
in the typical case that i and j are not chirality-flow connected to each other. If they are, we find for example



$$= 2p_1 \cdot p_2 \quad \text{[diagram with oval]} \quad , \quad (43)$$

i.e. we get back the chirality flow that we start with.

When describing the effect of spin-1 exchange, we also encounter structures with three momentum dots, for example while exchanging a photon between two fermions (i and j) which are chirality-flow connected with partners (i' and j'), in one case directly and in the other with a single momentum-dot in-between,



$$. \quad (44)$$

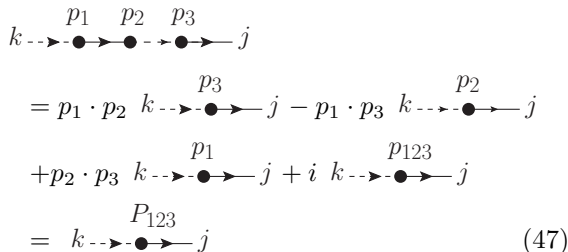
The line with three bullets represents the contraction $p_{1\mu}p_{2\nu}p_{3\rho}[i'|\sigma^\mu\bar{\sigma}^\nu\sigma^\rho|j']$ for the four-vectors p_1, p_2 and p_3 associated with the momentum-dots. To decompose this structure, we contract $\sigma^\mu\bar{\sigma}^\nu\sigma^\rho$ with $g_{\mu\nu}, g_{\mu\rho}, g_{\nu\rho}$ and $\epsilon_{\mu\nu\rho\alpha}$, giving a system of four equations and four unknowns with solution

$$\sigma^\mu\bar{\sigma}^\nu\sigma^\rho = g^{\mu\nu}\sigma^\rho - g^{\mu\rho}\sigma^\nu + g^{\nu\rho}\sigma^\mu + i\epsilon^{\mu\nu\rho\alpha}\sigma^\alpha, \quad (45)$$

corresponding to

$$\begin{aligned} & p_{1\mu} p_{2\nu} p_{3\rho} [k|\sigma^\mu\bar{\sigma}^\nu\sigma^\rho|j] \\ &= p_1 \cdot p_2 p_{3\rho} [k|\sigma^\rho|j] - p_1 \cdot p_3 p_{2\rho} [k|\sigma^\rho|j] \\ &+ p_2 \cdot p_3 p_{1\rho} [k|\sigma^\rho|j] + i \underbrace{p_{1\mu}p_{2\nu}p_{3\rho}\epsilon^{\mu\nu\rho\alpha}}_{P_{123\alpha}} [k|\sigma^\alpha|j], \end{aligned} \quad (46)$$

or in the momentum-dot notation (for general $[k]$ and $[j]$)



$$\begin{aligned} & k \dashrightarrow \bullet \xrightarrow{p_1} \bullet \xrightarrow{p_2} \bullet \xrightarrow{p_3} \bullet \dashrightarrow j \\ &= p_1 \cdot p_2 k \dashrightarrow \bullet \xrightarrow{p_3} \bullet \dashrightarrow j - p_1 \cdot p_3 k \dashrightarrow \bullet \xrightarrow{p_2} \bullet \dashrightarrow j \\ &+ p_2 \cdot p_3 k \dashrightarrow \bullet \xrightarrow{p_1} \bullet \dashrightarrow j + i k \dashrightarrow \bullet \xrightarrow{P_{123}} \bullet \dashrightarrow j \\ &= k \dashrightarrow \bullet \xrightarrow{P_{123}} \bullet \dashrightarrow j \end{aligned} \quad (47)$$

for

$$P_{123} \equiv p_1 \cdot p_2 p_3 - p_1 \cdot p_3 p_2 + p_2 \cdot p_3 p_1 + ip_{123}. \quad (48)$$

This means that we retrieve the structure of a single momentum-dot for some 'momentum' P_{123} .

For the action of a momentum-dot on our basic building blocks, the basis vectors, eq. (37) in the main text, we find by antisymmetrizing

$$\begin{aligned} & k \dashrightarrow \bullet \xrightarrow{[p_1, p_2] p_3} \bullet \dashrightarrow j \\ &= -p_1 \cdot p_3 k \dashrightarrow \bullet \xrightarrow{p_2} \bullet \dashrightarrow j + p_2 \cdot p_3 k \dashrightarrow \bullet \xrightarrow{p_1} \bullet \dashrightarrow j \\ &+ i k \dashrightarrow \bullet \xrightarrow{p_{123}} \bullet \dashrightarrow j \quad . \end{aligned} \quad (49)$$

In the general case, the contraction to the left is with a general antisymmetric rank-2 tensor $(A_{12})_{\mu_1\mu_2}$. In this case, defining

$$F_{[[1,2],3]\mu} = 2(A_{12})_{\mu\nu}p_3^\nu + i(A_{12})_{\mu_1\mu_2}p_{3\mu_3}\epsilon^{\mu_1\mu_2\mu_3\mu} \quad (50)$$

the decomposition reads

$$k \dashrightarrow \bullet \xrightarrow{A_{12} p_3} \bullet \xrightarrow{F_{[[1,2],3]}} \bullet \dashrightarrow j = k \dashrightarrow \bullet \xrightarrow{F_{[[1,2],3]}} \bullet \dashrightarrow j \quad . \quad (51)$$

The next structures to consider are those with a total of four contractions, either of form $\dashrightarrow \bullet \xrightarrow{\bullet} \bullet \xrightarrow{\bullet} \bullet \dashrightarrow$ (where the middle two dots come from a fermion propagator, and the outermost dots from the initial chirality flows containing one momentum dot each), of form $\dashrightarrow \bullet \xrightarrow{\bullet} \bullet \xrightarrow{\bullet} \bullet \dashrightarrow$ (from one initial chirality flow of type $\dashrightarrow \bullet \xrightarrow{\bullet} \bullet \dashrightarrow$, one or two momentum dots from a propagator, and (if one) the other from the initial chirality flow of the other involved fermion), or of form $\dashrightarrow \bullet \xrightarrow{\bullet} \bullet \xrightarrow{\bullet} \bullet \dashrightarrow$ (from an initial state of two boxes contracted with the mass term in the propagator).

For this decomposition, we first explore the antisymmetric part $\dashrightarrow \bullet \xrightarrow{\bullet} \bullet \xrightarrow{\bullet} \bullet \dashrightarrow$. Exploiting symmetries and fixing constants, this can be decomposed into

$$\begin{aligned} & i \dashrightarrow \bullet \xrightarrow{A_{12} A_{34}} \bullet \xrightarrow{\bullet} \bullet \xrightarrow{\bullet} \bullet \dashrightarrow j \\ &= [-2(A_{12})_{\mu_1\mu_2}(A_{34})^{\mu_1\mu_2} \\ &+ i\epsilon^{\mu_1\mu_2\mu_3\mu_4}(A_{12})_{\mu_1\mu_2}(A_{34})_{\mu_3\mu_4}] i \dashrightarrow \bullet \xrightarrow{\bullet} \bullet \xrightarrow{\bullet} \bullet \dashrightarrow j \\ &+ i \dashrightarrow \bullet \xrightarrow{A'_{[[1,2],[3,4]]}} \bullet \xrightarrow{\bullet} \bullet \dashrightarrow j \end{aligned} \quad (52)$$

where

$$A'_{[[1,2],[3,4]]\mu\nu} = 2 \left((A_{12})_{\mu\eta}(A_{34})^\eta{}_\nu - (A_{12})_{\nu\eta}(A_{34})^\eta{}_\mu \right) \quad (53)$$

is made manifestly antisymmetric since only the antisymmetric part survives the contraction. The result in eq. (52), along with eq. (41) and (and versions where dotted and undotted lines switch role) completes the set of

Kinematic expansions are performed around the physical mass shells of particles carrying a hard momentum, and include quasi-soft as well as other enhanced kinematic regions. The resulting factorization of physical, renormalized S-matrix elements accounts for color, isospin and spin correlations, as well as the proper wave function renormalization constants. Results of our formalism, together with suitable mappings which implement energy-momentum conservation, can directly be implemented in the `CVolver` evolution library [7, 9] and will serve as a basis to design parton branching algorithms which include electroweak effects beyond the quasi-collinear limit.

ACKNOWLEDGMENTS

We are thankful to Maximilian Löschner for fruitful discussions (in particular on the complex mass scheme)

and for a very careful reading of the manuscript. We are also thankful to Ines Ruffa for useful discussions. This work was supported by the Swedish Research Council (contract number 2016-05996, as well as the European Union’s Horizon 2020 research and innovation programme (grant agreement No 668679). This work has also been supported in part by the European Union’s Horizon 2020 research and innovation programme as part of the Marie Skłodowska-Curie Innovative Training Network MCnetITN3 (grant agreement no. 722104), and in part by the COST actions CA16201 “PARTICLE-FACE” and CA16108 “VBSCAN”. We are grateful to the Erwin Schrödinger Institute Vienna for hospitality and support while significant parts of this work have been achieved within the Research in Teams programmes “Amplitude Level Evolution II: Cracking down on colour bases.” (RIT0521).

-
- [1] S. Catani and M. Grazzini, Nucl. Phys. B **570**, 287 (2000), arXiv:hep-ph/9908523.
 - [2] J. R. Forshaw, J. Holguin, and S. Plätzer, JHEP **09**, 014 (2020), arXiv:2003.06400 [hep-ph].
 - [3] N. Kidonakis, G. Oderda, and G. Sterman, Nucl. Phys. B **531**, 365 (1998), hep-ph/9803241.
 - [4] H. Contopanagos, E. Laenen, and G. Sterman, Nuclear Physics B **484**, 303 (1997).
 - [5] G. Oderda, Phys. Rev. D **61**, 014004 (2000), arXiv:hep-ph/9903240.
 - [6] M. Sjö Dahl, JHEP **09**, 087 (2009), arXiv:0906.1121 [hep-ph].
 - [7] S. Plätzer, Eur. Phys. J. C **74**, 2907 (2014), arXiv:1312.2448 [hep-ph].
 - [8] R. Ángeles Martínez, M. De Angelis, J. R. Forshaw, S. Plätzer, and M. H. Seymour, JHEP **05**, 044 (2018), arXiv:1802.08531 [hep-ph].
 - [9] M. De Angelis, J. R. Forshaw, and S. Plätzer, Phys. Rev. Lett. **126**, 112001 (2021), arXiv:2007.09648 [hep-ph].
 - [10] S. Plätzer and I. Ruffa, JHEP **06**, 007 (2021), arXiv:2012.15215 [hep-ph].
 - [11] J. R. Forshaw, J. Holguin, and S. Plätzer, JHEP **08**, 145 (2019), arXiv:1905.08686 [hep-ph].
 - [12] M. Löschner, S. Plätzer, and E. S. Dore, (2021), arXiv:2112.14454 [hep-ph].
 - [13] P. Ciafaloni and D. Comelli, Phys. Lett. B **446**, 278 (1999), arXiv:hep-ph/9809321.
 - [14] A. Denner and S. Pozzorini, Eur. Phys. J. C **18**, 461 (2001), arXiv:hep-ph/0010201.
 - [15] A. Denner and S. Pozzorini, Eur. Phys. J. C **21**, 63 (2001), arXiv:hep-ph/0104127.
 - [16] P. Ciafaloni and D. Comelli, JHEP **11**, 022 (2005), arXiv:hep-ph/0505047.
 - [17] J.-y. Chiu, F. Golf, R. Kelley, and A. V. Manohar, Phys. Rev. Lett. **100**, 021802 (2008), arXiv:0709.2377 [hep-ph].
 - [18] A. V. Manohar and W. J. Waalewijn, JHEP **08**, 137 (2018), arXiv:1802.08687 [hep-ph].
 - [19] R. Kleiss and R. Verheyen, Eur. Phys. J. C **80**, 980 (2020), arXiv:2002.09248 [hep-ph].
 - [20] M. R. Masouminia and P. Richardson, (2021), arXiv:2108.10817 [hep-ph].
 - [21] H. Brooks, P. Skands, and R. Verheyen, (2021), arXiv:2108.10786 [hep-ph].
 - [22] J. Chen, T. Han, and B. Tweedie, JHEP **11**, 093 (2017), arXiv:1611.00788 [hep-ph].
 - [23] C. W. Bauer, N. Ferland, and B. R. Webber, JHEP **08**, 036 (2017), arXiv:1703.08562 [hep-ph].
 - [24] C. W. Bauer, D. Provasoli, and B. R. Webber, JHEP **11**, 030 (2018), arXiv:1806.10157 [hep-ph].
 - [25] S. Plätzer, JHEP **07**, 126 (2023), arXiv:2204.06956 [hep-ph].
 - [26] A. Manohar, B. Shotwell, C. Bauer, and S. Turczyk, Phys. Lett. B **740**, 179 (2015), arXiv:1409.1918 [hep-ph].
 - [27] F. Reiner and A. Maas, PoS **EPS-HEP2021**, 449 (2022), arXiv:2110.07312 [hep-ph].
 - [28] Effectively, the relation between kinematics and masses does force us to use pole masses despite they might not be optimal. Keeping track of renormalization factors and a controlled expansion we have, however, all information at hand to convert to different mass schemes.
 - [29] A. Denner and S. Dittmaier, Nucl. Phys. B Proc. Suppl. **160**, 22 (2006), arXiv:hep-ph/0605312.
 - [30] A. Denner and J.-N. Lang, Eur. Phys. J. C **75**, 377 (2015), arXiv:1406.6280 [hep-ph].
 - [31] S. Frixione and B. R. Webber, JHEP **11**, 045 (2021), arXiv:2106.13471 [hep-ph].
 - [32] J. R. Forshaw, J. Holguin, and S. Plätzer, (2021), arXiv:2112.13124 [hep-ph].
 - [33] S. Keppeler and M. Sjö Dahl, JHEP **09**, 124 (2012), arXiv:1207.0609 [hep-ph].
 - [34] J. Alcock-Zeiling and H. Weigert, J. Math. Phys. **58**, 051703 (2017), arXiv:1610.08802 [math-ph].
 - [35] M. Sjö Dahl and J. Thorén, JHEP **11**, 198 (2018), arXiv:1809.05002 [hep-ph].
 - [36] J. Alcock-Zeiling, S. Keppeler, S. Plätzer, and M. Sjö Dahl, J. Math. Phys. **64**, 023504 (2023), arXiv:2209.15013 [hep-ph].
 - [37] S. Keppeler, S. Plätzer, and M. Sjö Dahl, (2023), arXiv:2312.16688 [hep-ph].

- [38] A. Lifson, C. Reuschle, and M. Sjodahl, Eur. Phys. J. C **80**, 1006 (2020), arXiv:2003.05877 [hep-ph].
- [39] J. Alnefjord, A. Lifson, C. Reuschle, and M. Sjodahl, Eur. Phys. J. C **81**, 371 (2021), arXiv:2011.10075 [hep-ph].
- [40] A. Lifson, M. Sjodahl, and Z. Wettersten, Eur. Phys. J. C **82**, 535 (2022), arXiv:2203.13618 [hep-ph].
- [41] E. Boman, A. Lifson, M. Sjodahl, A. Warnerbring, and Z. Wettersten, JHEP **02**, 005 (2024), arXiv:2312.07447 [hep-ph].
- [42] A. Lifson, S. Plätzer, and M. Sjodahl, (2023), arXiv:2303.02125 [hep-ph].

APPENDIX

Appendix A: Propagators and external wave functions

An important ingredient to our factorization formula is to demonstrate, subject to the kinematic parametrization above, that

$$\sum_{n=0}^{\infty} \left(\frac{\mathbf{P}(q_i + K_{i,s}, M_i)}{(q_i + K_{i,s})^2 - \tilde{M}_{R,i}^2} \Sigma(q_i + K_{i,s}) \right)^n \frac{\mathbf{P}(q_i + K_{i,s}, M_i)}{(q_i + K_{i,s})^2 - \tilde{M}_{R,i}^2} = \frac{1}{2p_i \cdot Q_{i,s}} \frac{\Psi(\Lambda p_i, M_i) \bar{\Psi}(\Lambda p_i, M_i)}{1 - \Sigma'(M_i^2)} + \mathcal{O}(\lambda), \quad (\text{A1})$$

where the derivative of the (physical part of the) self-energy $\Sigma(p^2)$ (or, accordingly the transverse self-energy at vanishing k^2 for a massless boson) provides the proper wave function renormalization for the amplitude we factor to. To illustrate this let us first consider Goldstone bosons in an R_ξ gauge, with a free propagator $i/(k^2 - \xi \tilde{M}_{R,i}^2)$, where $\tilde{M}_{R,i}^2 = M_{R,i}^2 + iM_{R,i}\Gamma_{R,i}$ in a complex mass scheme [29, 30], and the introduction of $\Gamma_{R,i}$ needs to be added back as additional insertions of two-point functions. This does not provide any change to our main argument. The propagators of the physical scalar can be obtained by putting $\xi = 1$. If the scalar has a one-particle irreducible two-point function $-i\Sigma_S(k^2)$, the resummed propagator is

$$\frac{1}{(q_i + K_{i,s})^2 - \xi \tilde{M}_{R,i}^2 - \Sigma_S((q_i + K_{i,s})^2)} = \begin{cases} \frac{1}{2p_i \cdot Q_{i,s}} \frac{1}{1 - \Sigma'(M_i^2)} + \mathcal{O}(\lambda) & \xi = 1 \text{ and } \Sigma_S(k^2) = \Sigma(k^2) \\ \mathcal{O}(\lambda) & \text{otherwise} \end{cases} \quad (\text{A2})$$

where the physical and renormalized (complex) mass relate as $M_i^2 = \tilde{M}_{R,i}^2 + \Sigma(M_i^2)$ for the boson in question. This depending on how the unphysical scalar's self energy and the gauge parameter relate to each other, the scalars will contribute at leading power along with their related vector bosons, or not. We will investigate this in more detail in the future. The simplest non-scalar case to consider is that of a massive gauge boson. In an R_ξ gauge their numerator reads

$$V^{\mu\nu}(q_i + K_{i,s}, M_i) = -\eta^{\mu\nu} + (1 - \xi) \frac{(q_i + K_{i,s})^\mu (q_i + K_{i,s})^\nu}{(q_i + K_{i,s})^2 - \xi M_i^2}. \quad (\text{A3})$$

Using the momentum parametrization, eq. (3) in the main text, we have

$$V^{\mu\nu}(q_i + K_{i,s}, M_i) = -\eta^{\mu\nu} - \alpha^2(1 - \xi) \frac{(\Lambda p_i)^\mu (\Lambda p_i)^\nu}{2p_i \cdot Q_{i,s} + (1 - \xi) M_i^2} = \sum_{\lambda} \epsilon_{\lambda,M}^{\mu}(\Lambda p_i, M_i) \epsilon_{\lambda,M}^{*\nu}(\Lambda p_i, M_i) + \mathcal{O}(\lambda) \quad (\text{A4})$$

where the physical polarization sum is $\sum_{\lambda} \epsilon_{\lambda,M}^{\mu}(p_i, M_i) \epsilon_{\lambda,M}^{*\nu}(p_i, M_i) = -\eta^{\mu\nu} + p_i^{\mu} p_i^{\nu} / M_i^2$. At tree level and $\xi = 1$ this would not hold, but in this case the Goldstones would contribute, as shown above. For $\xi \neq 1$ we obtain the physical polarization sum, and the Goldstones would not contribute. The summed propagator is more complicated, however we still find that the above relation holds with the expected additional factor of the (complex) transverse self-energy of the respective boson, as claimed at the beginning of this section. For Fermions the propagator numerator is linear in the momentum and thus they trivially satisfy our constraints at leading power. The last complicated case is that of a massless gauge boson in physical gauge, for which we observe that

$$d^{\mu\nu}(q, n) = -\eta^{\mu\nu} + \frac{q^{\mu} n^{\nu} + n^{\mu} q^{\nu}}{n \cdot q} \quad (\text{A5})$$

which clearly satisfies

$$d^{\mu\nu}(q_i + K_{i,s}, n) = d^{\mu\nu}(\Lambda p_i) + \mathcal{O}(\lambda) = \sum_{\lambda} \epsilon_{\lambda}^{\mu}(\Lambda p_i, n) \epsilon_{\lambda}^{*\nu}(\Lambda p_i, n) + \mathcal{O}(\lambda) \quad (\text{A6})$$

where $\epsilon(q, n)$ are the physical transverse polarization vectors satisfying $\epsilon(q, n) \cdot q = \epsilon \cdot n = 0$ and $\epsilon_{\lambda}(q, n) \cdot \epsilon_{\sigma}(q, n) = -\delta_{\lambda\sigma}$. For a full propagator we get the usual renormalization factor $1/(1 - \Sigma_T(0))$ where Σ_T is the transverse part of the self energy, and the part which is longitudinal to the gauge vector is again only contributing at subleading power.